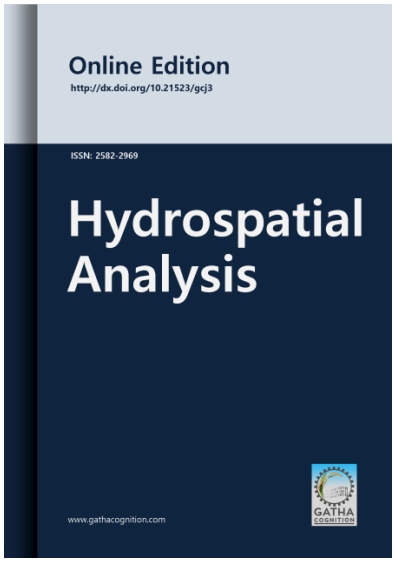

Hydrospatial Analysis

Editor-in-Chief: **Professor Pramodkumar Hire**

EISSN: 2582-2969

DOI: https://doi.org/10.21523/gcj3

Climate Change Impacts on LULC in the Jarmet Wetland and its Surrounding Areas in Western Ethiopia

Amanuel Kumsa Bojer[1*], Karuturi Venkata Suryabhagavan[2], Samson Tsegaye Mekasha[2], Ayad M. Fadhil Al-Quraishi[3]

1. Ethiopian Artificial Intelligence Institute, P.O.Box, 40782, Addis Ababa, Ethiopia.
2. School of Earth Sciences, Addis Ababa University, P.O. Box 1176, Addis Ababa, Ethiopia.
3. Petroleum and Mining Engineering Department, Faculty of Engineering, Tishk International University, Erbil, Iraq.

To cite this article

Bojer, A. K., Suryabhagavan, K. V., Mekasha, S. T. and Al-Quraishi, A. M. F., 2023. Climate Change Impacts on LULC in the Jarmet Wetland and its Surrounding Areas in Western Ethiopia. *Hydrospatial Analysis*, 7(1), 1-18.
DOI: https://doi.org/10.21523/gcj3.2023070101

GATHA COGNITION
https://gathacognition.com

Hydrospatial Analysis
Homepage: www.gathacognition.com/journal/gcj3
http://dx.doi.org/10.21523/gcj3

Original Research Paper

Climate Change Impacts on LULC in the Jarmet Wetland and its Surrounding Areas in Western Ethiopia

Amanuel Kumsa Bojer[1*], Karuturi Venkata Suryabhagavan[2], Samson Tsegaye Mekasha[2], Ayad M. Fadhil Al-Quraishi[3]

1. Ethiopian Artificial Intelligence Institute, P.O.Box, 40782, Addis Ababa, Ethiopia.
2. School of Earth Sciences, Addis Ababa University, P.O. Box 1176, Addis Ababa, Ethiopia.
3. Petroleum and Mining Engineering Department, Faculty of Engineering, Tishk International University, Erbil, Iraq.

Abstract

The concerns over land use and land cover (LULC) change have emerged on the global stage due to realization that changes occurring on the land surface also influence climate, ecosystem and its services. This study aimed to map the temporal dynamic of LULC patterns and LST in the Jarmet wetland in Ethiopia. The dynamics and pattern of changes for a period of 21 years (2000-2021) were analyzed using geospatial techniques. Multi-temporal satellite images from Landsat ETM$^+$ and Landsat-8 OLI sensor data were used to extract land-cover maps. The Land Surface Temperature (LST) trend of the study areas was computed using MODIS satellite imagery (2000-2021). Supervised classification using a Maximum Likelihood Classifier (MLC) was applied to prepare LULC maps of the watershed. The accuracy of the classified map was assessed using high-resolution data, and ground realities have been verified and ascertained through field observations. The results revealed a decreased trend in wetland, forest, shrubland and grassland in the period of 21 years (2000-2021) by -1148.71ha, -1073.26 ha, -1480.1 ha, and -87.73 ha, respectively. On the other hand, farmland and plantation areas followed an increasing trend. LST revealed decreasing trend in terms of mean and minimum with a fraction change of -0.018 and -0.073, whereas the maximum LST value shows an increasing trend with 0.021. The overall accuracy was 84.41%, with Kappa index of 76.13%. The analysis and findings of the study highlight important policy implications for sustainable LULC management in the study area. The study suggests the design and implementation of a guided natural resource policy, stopping the illegal expansion of farmland and educating society about the value of the sustainable management of habitat reserves.

Article History

Received: 24 October 2022
Revised: 07 December 2022
Accepted: 08 December 2022

Keywords

Climate;
Degradation;
Landsat;
LST;
Maximum Likelihood Classifier.

Editor(s)

P. Hire

1 INTRODUCTION

Land-use and land-cover (LULC) changes detection are vital for understanding the global environmental transform processes (Melakneh *et al*., 2010; Misrak *et al*., 2012; Ayele *et al*., 2014; RCW, 2018; Belete and Suryabhagavan, 2019; Mekasha *et al*., 2020; Bekele *et al*., 2022). Therefore, the detection and monitoring of LULC changes using satellite multi-spectral image data has been a topic of research interest in remote sensing (Mekasha *et al*., 2021). Mostly, human modify LULC types both quantitatively and qualitatively (FAO, 2016). Also, vegetation change affects precipitation and temperature, leading to climate change and global warming. In past studies, global environmental changes such as emissions of greenhouse gases, global climate change, loss of biodiversity and loss of soil resources have been closely linked to LULC changes (Mekasha *et al*., 2022). Increased climate variability and a warming trend in Sub-Saharan Africa, particularly East Africa, is due to exponential human population growth, irrational

* Author address for correspondence
School of Earth Sciences, Addis Ababa University, P.O. Box 1176, Addis Ababa, Ethiopia.
Tel.: +251-911998588
Emails: amanukumsa@gmail.com (*A. Bojer*); drsuryabhagavan@gmail.com (*K. Suryabhagavan* -Corresponding author); samson.tsegaye26@gmail.com (*S. Mekasha*); ayad.alquraishi@tiu.edu.iq (*A. Al-Quraishi*).

https://doi.org/10.21523/gcj3.2023070101

exploitation of natural resources, unabated forest destruction, extreme rainfall events and higher seasonal mean temperature (Costanza *et al*., 2014; Suryabhagavn, 2017).

Developing countries are the most affected by changes in climate and land-use. Various techniques of LULC change detection analysis were discussed by Mekasha *et al*. (2020). The impacts of human activities on wetlands can be manifested through LULC change. The LULC changes are the result of agricultural extension and population growth. Also, climate and land-use change contribute to natural disasters. Several studies justify this impact significantly by developing countries while limited resources, data, technology and budget for combating and resilience. However, the wetland is an inherently dynamic ecosystem that can be modified and destroyed by various natural processes, the direct and indirect consequences of human activity (Roy *et al*., 2010). Wetland degradation includes habitat loss and fragmentation, resource extraction, drainage and land reclamation, decline or extinction of wild flora and fauna, loss of soil nutrients, water resource, LULC changes are the result of a complex interplay of socio-economic, institutional and environmental factors (Turner *et al*., 1994; Tegene, 2002; Lesschen *et al*., 2005; Lambin and Geist, 2006; Falcucci *et al*., 2007; Li *et al*., 2017). According to Finlayson and Moser (1991) wetlands occupy about 6% (approximately 890 million ha) of the global land. However, about 50% of the world's wetlands have been altered or lost in the last 50 years (Dugan, 1993). In tropical and sub-tropical areas wetland conversion to alternative LULC since the 1950s was accelerated mainly due to agricultural land expansion and population growth (Moser *et al*., 2015). Wetlands of Africa only cover 1% (345000 km^2) of the total area of the continent. The total area of Ethiopia covers 113000000 ha (1130000 km^2) of land. In Ethiopia, more than 85% of the population lives in rural areas depending on agriculture as the main source of employment. Ethiopian highlands produce in excess of 110 billion meter cubic of water, of which 74% of the total volume of the water resource flows into rivers draining to Sudan, Egypt, Kenya, and Somalia (EPA, 2004; WBISPP, 2005). Therefore, it has attracted wide interests in communities of environment, geography, ecology, hydrology, GIS, remote sensing and so forth. The accuracy of predict LULC change depends on our ability to understand the precedent, contemporary and future drivers of LULC Change (Belete and Suryabhagavan, 2019; Mekasha *et al*., 2020). An improved understanding of historical LULC change patterns provides a better means to project future trends of LULC change (Melakneh *et al*., 2010; Misrak *et al*., 2012; Ayele *et al*., 2014; Mekasha *et al*., 2022).

Satellite remote sensing has the potential to provide accurate and timely geospatial information describing changes in LULC (Foody, 2002; Yuan *et al*., 2005). Among various earth observation (EO) programs NASA's Landsat missions are known for the free dissemination of extensive data. With the longest (since 1972) continual global coverage at moderate to high resolution, the Landsat data has been commonly used for LULC change detection (Helmer *et al*., 2000; Lu and Weng 2007; Gao and Zhang, 2009; Gumma *et al*., 2011; Lu *et al*., 2012; Jia *et al*., 2014; Mekasha *et al*., 2020). Remote sensing images can effectively record land-use situations and provide a good data source. From which updated LULC information and changes can be extracted, analyzed and simulated efficiently through certain means (Belete and Suryabhagavan, 2019). Several techniques for LULC changes have been reviewed (Lu *et al*., 2007). LULC change detection generally employs one of two basic methods: pixel-to-pixel comparison and post-classification comparison (Ayele *et al*., 2014; Dinku and Suryabhagavan, 2019), which compares two or more separately classified images of different dates (Shalaby and Tateishi, 2007; Serra *et al*., 2008). Post classification comparison is considered the more appropriate and commonly used method for change detection (Lillesand *et al*., 2004). Therefore, remote sensing is widely used in detecting and monitoring land use at different scales (Yuan *et al*., 2005).

Jarmet wetland witnessed drastic LULC changes mainly as a result of increase in changes in agriculture practices and execution of different development projects particularly during the last four decades. Geographic Information System (GIS) and Remote Sensing (RS) have proved to be very significant in analyzing and assessing LULC changes as well as LST (Melakneh *et al*., 2010; Misrak *et al*., 2012; Ayele *et al*., 2014). Satellite-based RS has the ability to provide synoptic LULC data at a specific time and location (Gomez *et al*., 2016; Verma *et al*., 2020). The RS and GIS have a remarkable ability to map and identify LULC and LST changes (Bekele *et al*., 2021). Over the last few decades, research studies highly relied on the satellite remote sensed spatial information to map individual vegetation species (Belete and Suryabhagavan, 2019) and describe the variation in the vegetation types (Warkaye *et al*., 2018; Bekele *et al*., 2022). The present study was taken up to investigate annual changes in LULC pattern and climate impact over the last three decades in Jarmet wetland and its surrounding environments in western Ethiopia by integrating remote sensing and GIS.

2 MATERIAL AND METHODS

2.1 Study Area

The current study was carried out at Jarmet wetland and surrounding environments located in western part of Ethiopia bounded by 9°52'43"-9°42'11"N latitude and 36°57'31"-37°05'50" E longitude covering a total area of 8113 ha (Figure 1). Elevation of the region ranges from 1781-2604 m. This wetland is flooded during rainy season and gradually dries up. It is part of the Blue Nile watershed which encompasses the Ethiopian renaissance dam. The climate of Ethiopia is mainly controlled by the

seasonal migration of Inter-Tropical Convergence Zone (ITCZ), which follows the position of the sun relative to the earth and the associated atmospheric circulation, in conjunction with the complex topography of the country (NMSA, 2019). Average annual temperature in the region is 27.7°C. Annual rainfall ranges between 411.9-334.6 mm with precipitation throughout the year, but mostly 85% between July and August. In Jarmet station the mean monthly highest temperature is recorded from February to April with its average 26.6°C and peak is 33.1 in February for this station (Figure 2). Vegetation is the assemblages of plant species and all ground cover by plants and the main elements of biosphere. Even though the study area is dominated by wetland surrounded by moist afro-montane forest, the remnants of mixed forest exist at the region in a portion of the study area. There are still mature individual plants of Olea Europea subs. cuspidata, Cordia Africana, Podocarpus falcatus, Ficus sycomorus, Phoenix reclinata, Syzygium guineense, Croton macrostachyus and Ficus vasta scattered are seen.

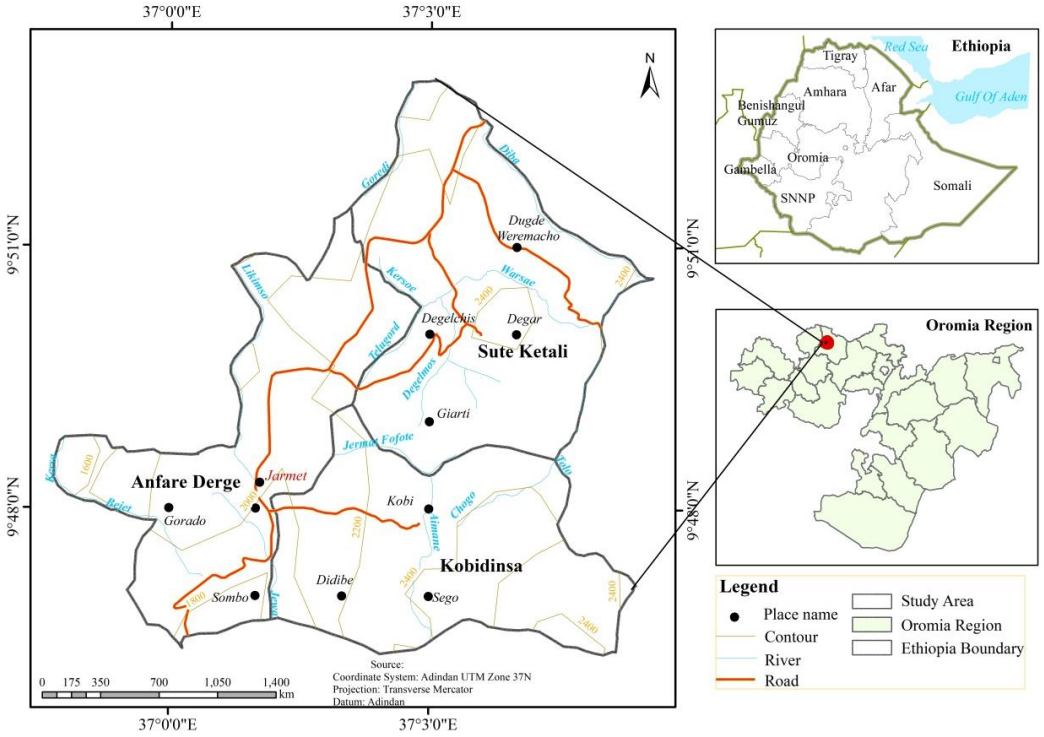

Figure 1. Study area: Jarmet wetland, Western Ethiopia

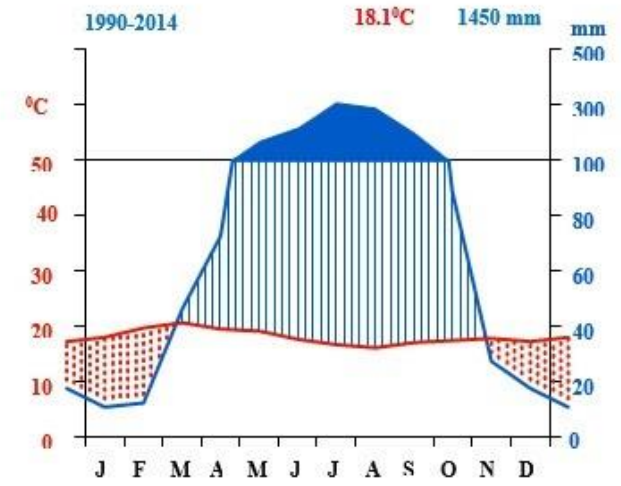

Figure 2. Precipitation

2.2 Data Acquisition

In this study, temporal data of three Landsat satellite remote sensing images such as Multispectral Scanner (MSS), Thematic Mapper (TM) and Enhanced Thematic Mapper Plus imageries for 2015, 2000, and 2021 used in this study were retrieved from the United State Geological Survey (USGS) database. Specifications of the satellite data acquired for change analysis are given in Table 1. The satellite images were projected in UTM projection, zone 37N and Adindan datum. Overall methodological framework and data analysis are presented in Figure 3.

2.3 Image Processing

The remote sensing image data of the years 2015, 2000, and 2021 were radially calibrated and atmospherically corrected. The relative geometric corrections of the four images were conducted to remove geometric distortion caused by sensor or the Earth's rotation. Due to the differences between the MSS and ETM$^+$ sensors, the geometric correction of the year 2000 was based on the data of the study area and the image georeferencing accuracy was initially checked with a reference map for the area. All the input images have the same map and projection information with the same number of layers. After layer stacking, sub-setting was performed to get a portion of a large image file into one smaller file. This is helpful to reduce the size of the image file and thus we could focus on only the area of interest.

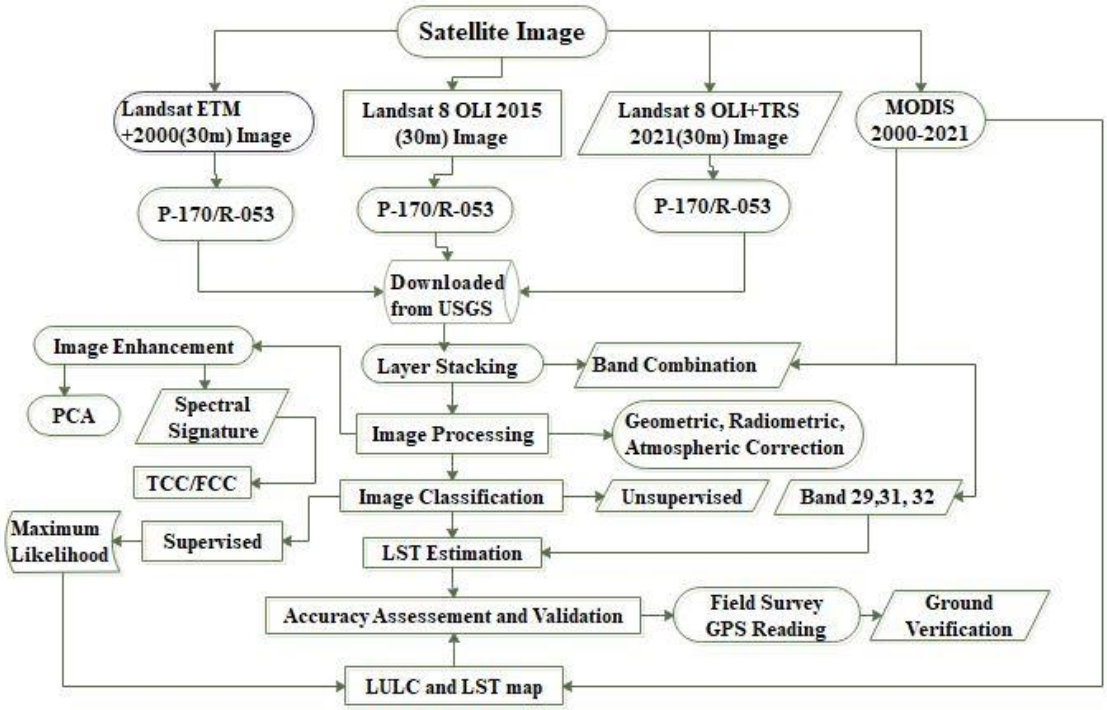

Figure 3. Methodological workflow

Table 1. Satellite imagery and data

Data type	Format	Path/row	Spectral bands	Scene size	Date of acquired and source	Resolution (m)
Topographic maps	Analogue	Sheet no.0937			January1982 to october1983 EMA	1:50000
Landsat TM	Digital	170/053	1,2,3,4,5,7	185×185 km	01-03-1986 USGS	30 m
Landsat ETM+	Digital	170/053	1,2,3,4,5,7	185×185 km	01-04-2000 USGS	30 m
Landsat ETM+	Digital	170/053	1,2,3,4,5,7	185×185 km	01-31-2005 GLCF	30 m
Landsat ETM+	Digital	170/053	1,2,3,4,5,7	185×185 km	02-11-2015 GLCF	30 m
Landsat MSS	Digital	182/053	1,2,3,4	185×185 km	12-09-1972 USGS	60 m
Geological maps	Analogue	Sheets: NC-37/9			August,2000 (GSE)	1:250000
MODIS LST	Digital	MOD11A2	36	2330km× 2330km	2000-2021	1 km

2.4 Image Classification

The overall objective of the digital image classification procedures is to automatically classify all pixels in an image into land classes or themes (Lillesand *et al*., 2004). It is a powerful technique to drive thematic classes from multiband image data. It performed for extraction of distinct classes or themes, LULC categories from satellite imagery. For this study, among the various classification methods, supervised and unsupervised classification procedures were used for satellite image classification. In order to minimize the biasness caused by using different band combinations, the same numbers of bands (band 2, 3, 4 and 5) were used for classification in all cases. In this study, training and validation data during optimization were generated using polygon vectors designed for each land-cover type. For the selection of land-cover types, supervised classification method of maximum likelihood algorithm training based region of interest mapping was used and 6 classes were determined from 2015, 2000, and 2021 Landsat satellite imagery. These classifications were produced by using ERDAS Imagine 2015, before the field work. This method is the most common method and widely used for supervised classification in remote sensing image data analysis (Richards, 2014). The maximum likelihood classification assumes that for all classes and the input data in each band follows the Gaussian (normal) distribution function. A pixel has a certain probability of belonging to a particular class. These probabilities are equally identifying and locate land-cover types that are known a priori through combination of personnel experience interpretation of satellite images, map analysis and field works (Jensen, 2005). Table 2 shows the present study and land use types of the study area. In order to model temporal changes in land cover were calculated and analyzed based on the formula of (Al-Naimi *et al*., 2017) as follows:

$$\text{Annual change rate(ha/yr)} = \frac{(a_2 - a_1)}{N} \quad (1)$$

where, annual change rate is the change in LULC (a_2–a_1), a_2 is the recent year land-use land-cover in ha, a_1 is the initial year LULC in ha and N is the number of years between the initial and the final of the study period. To compute percentage changes in each land-use and land-cover for the study area, targeted LULC were segmented into two change periods of image analysis. From equation (1), a relationship for estimating percentage change of targeted land-use and land-cover for the change detection periods understudy was established (2) (Al-Naimi *et al*., 2017).

$$\%\Delta inl = \frac{(a_2 - a_1)}{A} \times 100 \quad (2)$$

where, Δinl is a change in the targeted LULC understudy, a_1 and a_2 are the areas (image-based estimated areas) of the targeted land-use land cover at the beginning and end of the change detection analysis, and A is the total sum area.

2.5 Accuracy Assessment

Accuracy assessment is essential for individual classifications if the classification data is to be useful in change detection. LULC classification is subject to incur some errors; hence the output (maps) needs to be put to test for assessing accuracy using a reliable statistical technique. For that reason, LULC maps are usually accompanied by an accuracy assessment index that includes a clear description of the sampling design (including sample size and, if relevant, details of stratification), an error matrix, the area or proportion of area of each category according to the map, and descriptive accuracy measures such as user's, producer's and overall accuracy (Olofsson *et al*., 2013). The term 'accuracy' is typically used to express the measure of 'correctness' of a derived map (classification) which is assessed through the construction of error-matrix (Foody, 2002). To evaluate the accuracy of an image classification, it is a regular practice to create a confusion matrix. In a confusion matrix, the classification results are contrasted with additional reference (Google maps) data. The quality of a confusion matrix is that it distinguishes the nature of the classification errors and also their quantities. Frequently, surrogates to ground truths are obtained from existing land cover data (e.g., LULC map) which

Table 2. Land-use and land-cover classification scheme

LULC classes	Description
Wetland	The area where the water table is near or above the land surface covered by marshes, swamps, bogs, rivers and streams.
Forest	These areas are regions covered with big trees of different species, with little or no human activities.
Farmland	This class represents growing agricultural crops and appeared cultivated during growing season.
Shrubs	Areas covered with small shrubs, thickets and grasses with little or no trees are referred to as shrubs and its height is less than 5 m.
Plantation	This class includes eucalyptus plantation and temporary clear field stand a waiting replanting within in eucalyptus plantation.
Grassland	This category is dominated by the grasses, fobs, and grass areas used for communal grazing.

are perceived as suitable reference and which obviously are independent of the sample selection data. Classification accuracy could be affected by lack of fine details, resolutions of images used, due the need to make generalizations and errors are always expected accordingly. In this study accuracy assessment was done for recent satellite image of Landsat ETM$^+$ 2015 for which the ground truth data is likely corresponding. Error matrix is one of the most common methods of expressing classification accuracy (Congalton, 2009). An error matrix is square array of numbers set out in rows and columns which express the number of sample units (i.e., pixels, cluster of pixels, or polygons) assigned to a particular category relative to the actual category as verified on grounds. In the present study accuracy of all the raster layers (2015, 2000, and 2021) was assessed through the development of an error-matrix. A stratified random sampling design was adopted in the accuracy assessment.

The k (KHAT) statistic is a measure of the difference between the actual agreement between reference data and an automated classified data and the chance agreement between the reference data and a randomly classifications (Jensen, 2007). Conceptually, Ḱ can be defined as:

$$K = \frac{N\sum_i^r Xii - \sum_i^r (Xi*X+i)}{N^2 - \sum_i^r (Xi+*X+i)} \quad (3)$$

where, *N* is the total number of samples in the matrix, *r* is the number of rows in the matrix, *xii* is the number of observations in row *i* and column *i*, x_{+i} represent the total for row *i*, and x_{i+} represent the total for column *i*.

Table 3 shows the accuracy level of each land cover category of Landsat ETM$^+$2015. The error matrix can be used to determine the user and the map producer accuracy. The map producer accuracy is obtained by dividing the number of successes in the class by the total number of samples in a reference class (column). Map producer accuracy is an indicator of the omission errors. User accuracy is obtained by dividing the number of successes by the total number of samples in an obtained class (rows). User accuracy indicates the commission errors. This process is one of the widest and most commonly used validation methods for image classification either using open source or privative tools (Chuvieco, 2007; Lellisand *et al*., 2015). Validation using error matrix requires representative samples of the population to be assessed. In this study, the samples were determined using the multinomial distribution proposed by Congalton and Green (2009) (3). Small polygons were randomly selected and stratified as sampling unit. The classes were considered deferent amongst them (strata), but with great homogeneity respecting their use. The samples were determined from a chi-square distribution, using a confidence level of 95% and the percentage value of the image covered by each class. The current study revealed an overall accuracy of 84.06% with Kappa index of agreement of 0.75. This was reasonably a good overall accuracy and accepted for subsequent analysis and change detection. Sabins (1997) says that accuracy levels of more than 80% are considered adequate enough for reliable classification of land-cover types.

2.6 LST Retrieval

Satellite data is an essential data source used to derive LSTs, having the advantages of high quality, fine resolution and favorable spatiotemporal continuity (Belete and Suryabhagavan, 2019). LST is one of the important parameters in the study of surface energy balance. The commonly used methods of remote sensing inversion of LST mainly include the radiative transfer equation method, single window algorithm, single channel algorithm and split window algorithm (Wan *et al*., 2004). MODIS dataset originally found in sinusoidal (SIN) mapping grid and provided in the form of HDF (Hierarchical Data Format). Therefore, HDF format should be changed into Geotiff format to carry out further analysis. MODIS Land Surface Temperature/Emissivity (LST/E) data with 1 km spatial resolution with a data type of 16-bit unsigned integer to

Table 3. The accuracy level of each land-cover category of Landsat ETM+

Classified data	Reference data						Row total	OE (%)	UA (%)
	Shrubland	Grass land	Forest	Plantation	Wetland	Farmland			
Shrubland	4	0	0	0	0	0	4	2	100
Grassland	0	25	1	2	0	2	30	25	83.3
Forest	0	0	4	0	1	0	5	2	80
Plantation	0	2	0	11	0	0	13	15.4	85
Wetland	1	0	0	0	5	1	7	17	71
Farmland	0	2	0	0	0	16	18	15.8	88.9
Column total	5	29	5	13	6	19	77		
Commission Error (%)	0	16.7	2	15.40	29	11.11			
Producer Accuracy (%)	80	86.2	80	84.62	83	89			

Overall classification accuracy is 84.41 %, overall Kappa statistics is 0.76.

get the temperature data in °C (Sruthi and Mohammed, 2015). The pixel value (PV) of LST data is converted to °C by using the following empirical formula.

$$\text{LST}(°\text{C}) = (\text{PV} \times 0.02) - 273.15 \quad (4)$$

where *LST* is land surface temperature in degree centigrade (°C) and *PV* is pixel value of MODIS data.

3 RESULTS

3.1 LULC Change (2000-2021)

From visual and digital interpretations of the satellite imagery, different LULC categories were distinguished for this study. For the purposes of measurement of areal extent of Jarmet wetland and its surrounding environment; the satellite images were interpreted and analyzed and classified into six different classes. The areal extent of these land-use features is depicted in (Table 4 and Figure 4). The total areas of each LULC class of the study area were computed for five different periods from 2000 to 2021 farmland, wetland, shrubland and forestland were the major LULC types that have accounted for 30.5%, 15.9%, 20.46%, and 14.84%, of total study area. From 2000 to 2021, the wetland and its surrounding environment has dynamically transformed into different LULC categories. One of the most marked changes were the rapid decline of wetland and forested lands from 17.7% in 2000 to 3.5% in 2021 and from 23.8% in 2000 to 10.6% 2021, respectively. This was mainly due to dramatic expansion of farmland and plantation towards wet and forest lands. The farmland had occupied 30.8% of the study area in 2000 and increased to 58 % in 2021. Similarly, plantation cover has increased from 4.3% in 2000 to 19.5% in 2021. However, the other LULCs such as grass and shrub lands have shown irregular trend (increment at one period and decrement at other) over the study periods shown in (Figure 5).

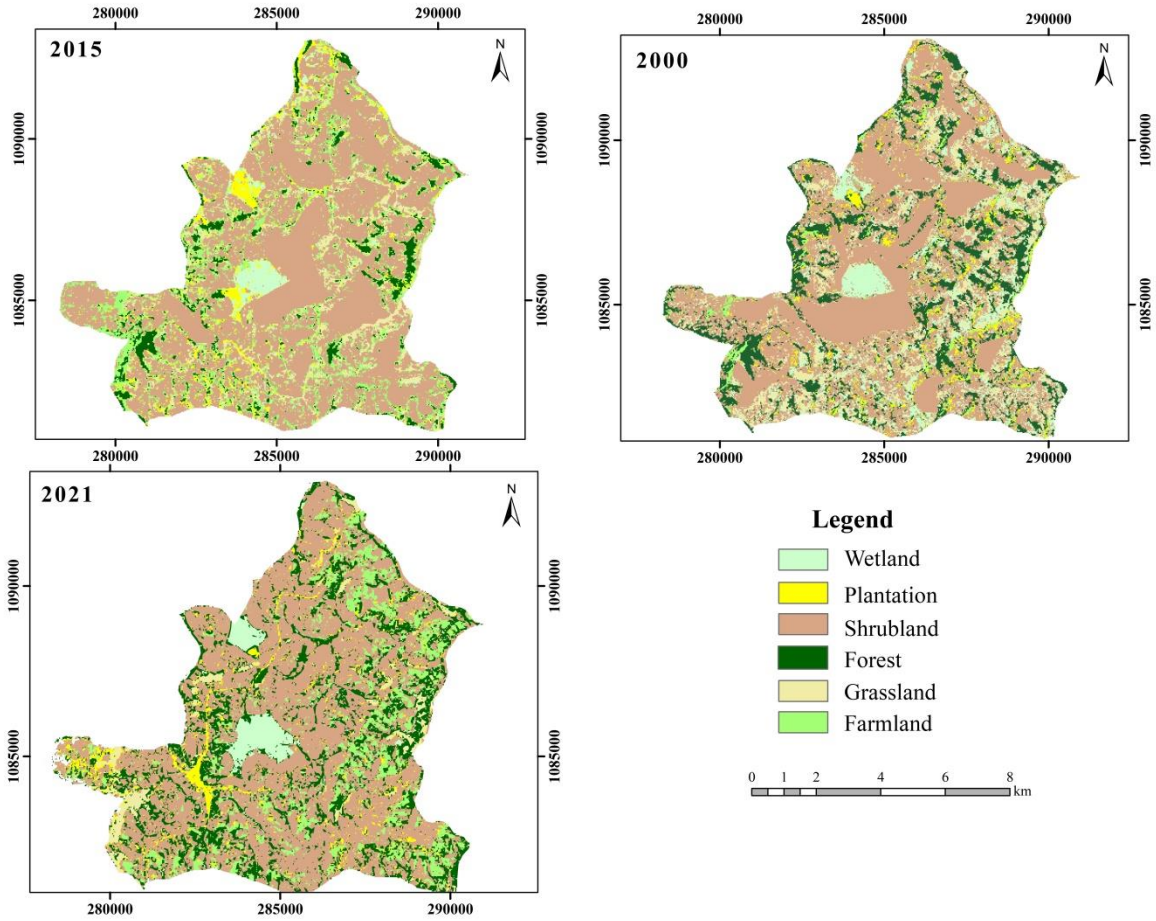

Figure 4. Land-use and land-cover maps

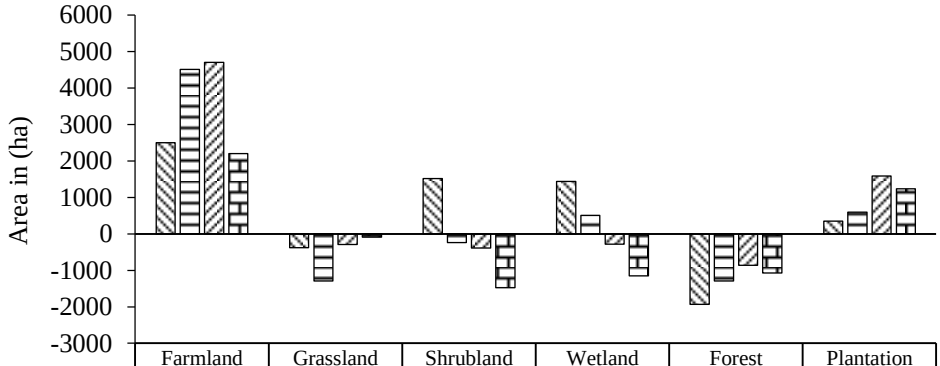

	Farmland	Grassland	Shrubland	Wetland	Forest	Plantation
2000	2495.48	-382.89	1518.38	1435.78	-1932.29	348.39
2015	4510.688	-1291.415	-237.478	505.831	-1291.415	591.333
2021	4,700.91	-295.17	-385.30	-287.29	-859.04	1585.32
Total area Δ(ha)	2205.41	-87.73	-1480.1	-1148.71	-1073.26	1236.92

Figure 5. Relative changes in LULC

Table 4. LULC changes during 2000-2021

LULC	2000		2015		2021		Net change	
	Area		Area		Area		Area	
	ha	%	ha	%	ha	%	ha	%
Shrubland	+1518.4	18.7	−237.5	2.9	−385.3	4.7	−1480.1	20.46
Farmland	+2495.5	30.8	+4510.8	55.6	+4700.91	58	+2205.41	30.5
Plantation	+348.4	4.3	+591.3	7.3	+1585.32	19.5	+1236.92	17.1
Forest	−1932.3	23.8	−1291.4	15.9	−859.04	10.6	−1073.26	14.84
Grassland	−382.9	4.7	+976.5	12.1	−295.17	3.6	−87.73	1.21
Wetland	+1435.8	17.7	−505.8	6.2	−287.29	3.5	−1148.71	15.9
Total	8113.3	100	8113.3	100	8133.3	100	8113.3	100

Note: The positive sign (+) means gain and the negative sign (−) indicates loss in areal extent.

3.2 LULC Spatiotemporal Patterns

Table 5 describes the land-use and land-cover trend and rate of changes of the study area during the period 2000-2021. Further, the results of LULC classes and their spatial distribution, there were changes showing decrease or increase in any particular LULC types. The LULC categories, which decreased are forest, wetland, grassland, and shrubland which contributed to concomitant increased of farmland and plantation. From 2000-2015, the forest land has decreased by about 42.72 ha at 11.23% rate per annum (Table 5 and Figure 6). Forest area during 2015-2021 rate of change per annum about 432.36 ha were converted by 16.22%. Various extents of forest cover existed in 2015 reduced by −1,073.26 ha (15.6%) during the period of 2015-2021 rate of change per annum. This revealed that the forest decreased is as a result of population growth, unwise use of resource and the forest resources change to other land units. From 2000 to 2021, the shrubland cover of the study areas has experienced the expansion of its spatial cover due to its encroachment into the wetlands and at the expense of the grass land covers. In addition, afforestation and reforestation conducted in the area have played great role in the expansion of shrubland. Furthermore, the number of livestock from time to time and conversion of grasslands and rangelands to agriculture created livestock pressure on existing grasslands and rangelands.

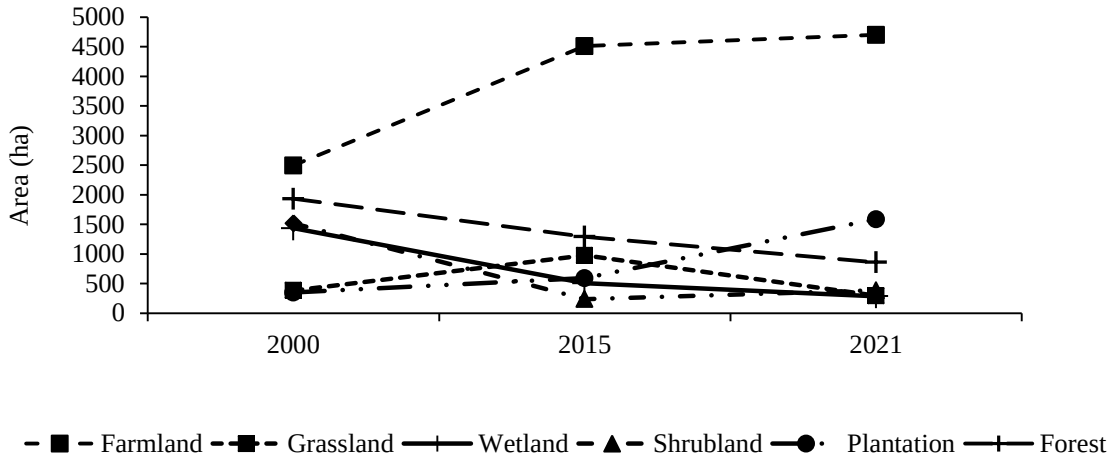

Figure 6. Temporal patterns of LULC

Table 5. LULC trends and annual changes during 2000, 2015 and 2021

LULC classes	2000-2015		2015-2021		2000-2021		Annual rate of change 2000-2021	
	Area		Area		Area		Area	
	ha	%	ha	%	ha	%	ha	%
Farmland	+2,015.30	35.33	+190.11	7.13	+2,205.41	32.03	+105.01	5.0
Wetland	−930.00	16.3	−218.51	8.2	−1,148.51	16.7	−4.2	0.2
Grassland	+593.60	10.4	−681.33	25.6	−87.73	1.3	−54.7	2.6
Shrubland	−1280.9	22.45	+147.8	5.54	−1,133.10	16.45	−53.95	2.56
Plantation	+242.90	4.25	+994.02	37.31	+1,236.92	17.96	+58.9	2.8
Forest	−640.90	11.23	+432.36	16.22	−1,073.26	15.6	−51.1	2.43

3.3 LULC Change Detection

The nature of land-use and land-cover change refers to the modification or conversion of LULC to other. A post classification comparison of annual changes revealed different trends in LULC changes from 2000-2021. This information serves as a vital tool in resource management decisions. This process involves a pixel-to-pixel comparison of images of the study years through overlay analysis. The nature of changes has been examined with reference to areas of LULC remained unchanged, gained from other classes and lost to other classes. LULC change during the study period is shown in Table 5.

From 2000 to 2021, the major LU/LC changes were dominated by the conversion from wetland, shrubland and grassland to farmland tabulated in (Table 6). Quantitatively, 1148.51ha, -1133.10ha and -87.73ha of wetland, shrubland and grassland were respectively converted to farmland. These changes were attributed to population growth which forced the farmers to till and expand their lands in greater extent than before to cope up the demand of the growing population and sustain their life. The land cover remained unchanged over the period of 43 years: 28 ha, 312 ha, 567 ha, 19 ha, 261 ha, and 371 ha were under the cover of shrubland, grassland, forest, plantation, wetland and farmland, respectively. Overall, 1558 ha (19.43%) of the total study area remained unchanged 2000-2021 during 43 years period. The change detection matrix as well indicated that there was gain in farmland and plantation area coverage by 1.67 km^2 (167 ha) and 1.41 km^2 (141 ha) respectively, whereas grassland, shrubland, wetland and forest lands showed decline (loss) in their areal extent by -641 ha, -1,701 ha, -1,713 ha, and -294 ha, respectively.

3.4 The Impact of LULC Change on Climate

Climate data monthly average for rainfall and temperature statistical mean values or long-term

averages were calculated in Diva GIS and presented using graphs. Analyses on generating the average rainfall and temperatures were conducted to reveal general information on the overall estimated rainfall values over a period of 20 years. The study area was observed to have two rainfall seasons the long-term March, April and May season and the short-term rainfall June, July and August as per the rainfall pattern in Figure 7. The highest rainfall amounts were seen in 2000 at 280 mm for 300 mm for the JJA [June, July, and August] season during 2020. 2000 had the minimal rainfall during the MAM [March, April, and May] season at 150 mm and mm for the year 2020 during the MAM season. As observed in the seasonal rainfall variability graph in Figure 7, there was much variability in rainfall especially in the year 2020 which has the highest variability of 25% recorded during the long rains (MAM) and a high of 48% for the short rains season (JJA). This was evident from the field questionnaires where most of the people agreed that there was a huge variability in season and late onsets of rainfall especially during the JJA rainfall season.

3.5 Climatic Parameters of the Jarmet Wetland

In the Jarmet wetland, annual average rainfall decreased by 12 mm between 2000 and 2020 (Figure 8). Annual average temperatures also increased between 2000 and 2020 by 1.5°C. The average annual temperature was 24.5°C before 2001, and raised to27.3°C after 2001. The error bar maps the confidence interval of the forecast at 95%. Figure 9 depicts the average annual temperatures during 2000-2020 and annual diurnal temperature for the year 2020. A simple annual vapor of precipitation and diurnal temperature for 20 years was performed using the available data. The results are statistically acceptable with a symmetric mean absolute percentage error (SMAPE) of 0.13 and 0.01 for precipitation and temperature, respectively. The graph of forecast for the year 2020 showed a decrease in precipitation of 18% and 10% as compared to the mean precipitation of the periods 2000-2015 and 2015-2020, respectively. As for the temperature, an increase of 18.5% ºC is predicted for the year 2000, as compared to the initial mean temperature of 17.0°C for the period 2000. There is also a strong inter-annual variability in wind speed, with a decreasing trend between 2000-2010 and 2010-2020 (Figure 10).

3.6 Land Surface Temperature Trends

Figure 11 and 12 indicates a spatial pattern and areal distribution of LST in 2000 to 2021 of the Jarmet Wetland. The land surface temperature has shown that decreasing trend of mean and minimum LST with a changing factor of -0.018, -0.073 whereas maximum LST show increasing trend with 0.021 changing factor. Accordingly, the result show that mean, minimum and maximum LST varied from 25.68°C, -29.97°C, 6.97ºC -15.95ºC and 39.61ºC -46.99ºC, respectively (Table 7).

Table 6. Change matrix of land-use/land-cover changes between 2000 and 2021

		Initial State 2000													
		SHL		GL		FR		PL		WL		FL			
	LULC	Area		Area		Area		Area		Area		Area		RT	CT
		ha	%	ha	%	ha	%	ha	%	ha	%	ha	%		
Final state 2021	SHL	28	1.4	78	4.8	33	2.1	1	0.6	88	4	8	1.5	236	244
	GL	208	10.7	312	19.2	101	6.3	8	5	321	14.4	21	3.9	971	988
	FR	143	7.3	125	7.7	567	35.5	16	0.1	298	13.4	105	19.5	1253	1302
	PL	358	18.4	35	2.1	116	7.3	19	11.9	47	2.1	24	4.5	599	600
	WL	52	2.7	19	1.2	165	10.3	0	0	261	11.7	7	1.3	504	511
	FL	1,153	59.2	1052	64.6	575	36.3	16	0.1	1186	53.3	371	69	4454	4493
	CCT	1,946	100	1629	100	1596	100	160	17.7	2225	100	538	100	8017	8111
	CC	1,918	98.6	1317	80.8	1029	64.5	141	88.1	1964	88.3	168	31.2		
	ID	-1701	-87.4	-641	-39.3	-294	-18.4	439	2.7	-1713	-77	3954	735		

Note: Land-cover categories are SHL: Shrubland, GL: Grassland, FR: Forest, PL: Plantation, WL: Wetland and FL: Farmland, RT: Row total, CC: Class Change, CT: Class total, ID: Image difference, CCT: Column class total.

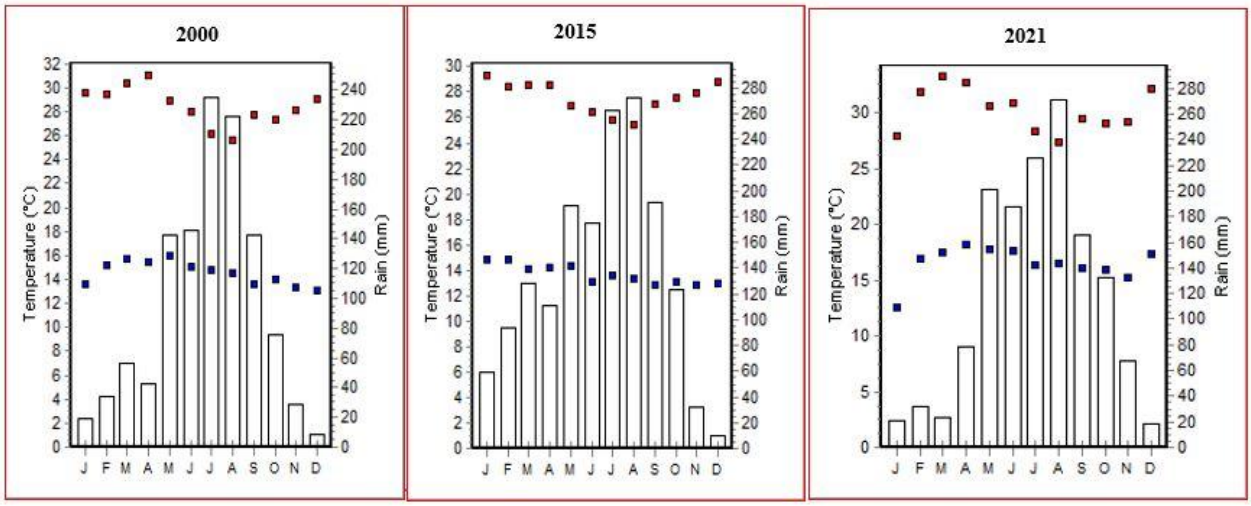

Figure 7. Predicted rainfall and temperature

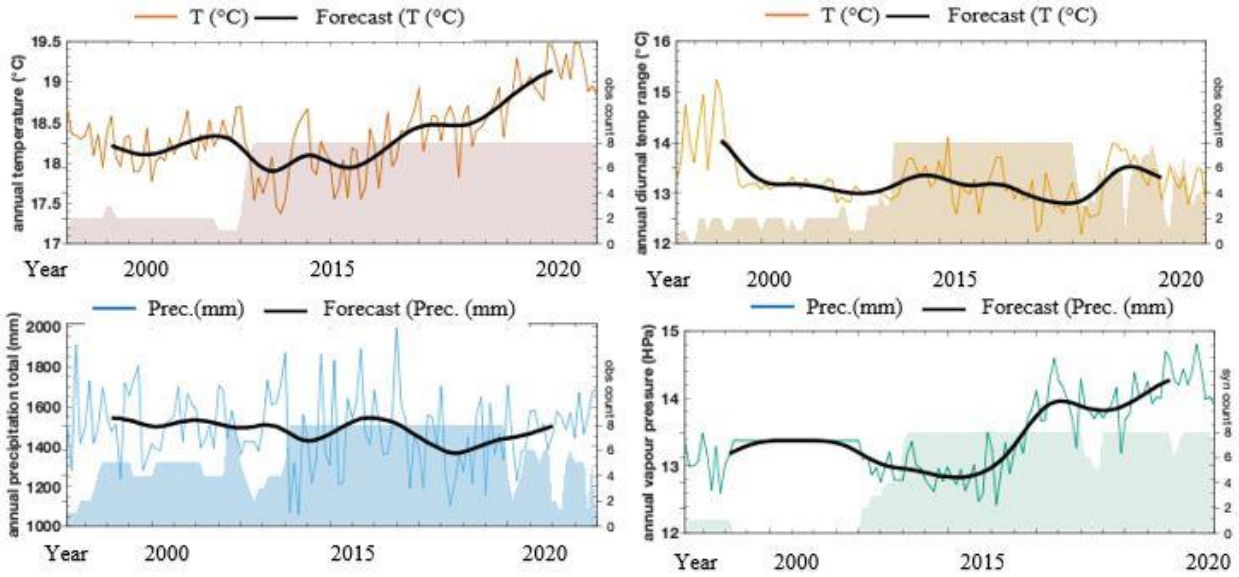

Figure 8. Annual and diurnal rainfall and temperature

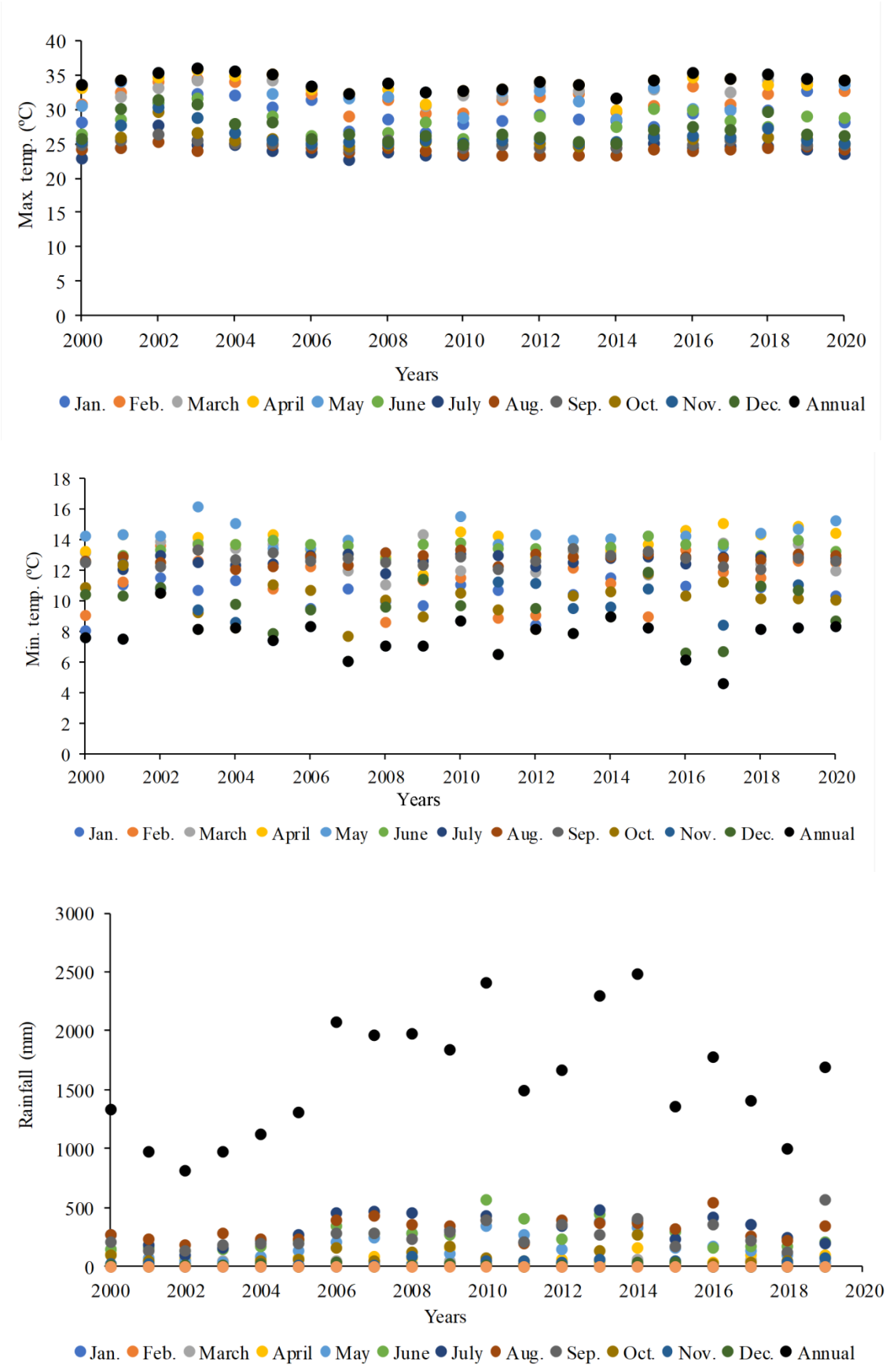

Figure 9. Temperature and rainfall during 2000-2020

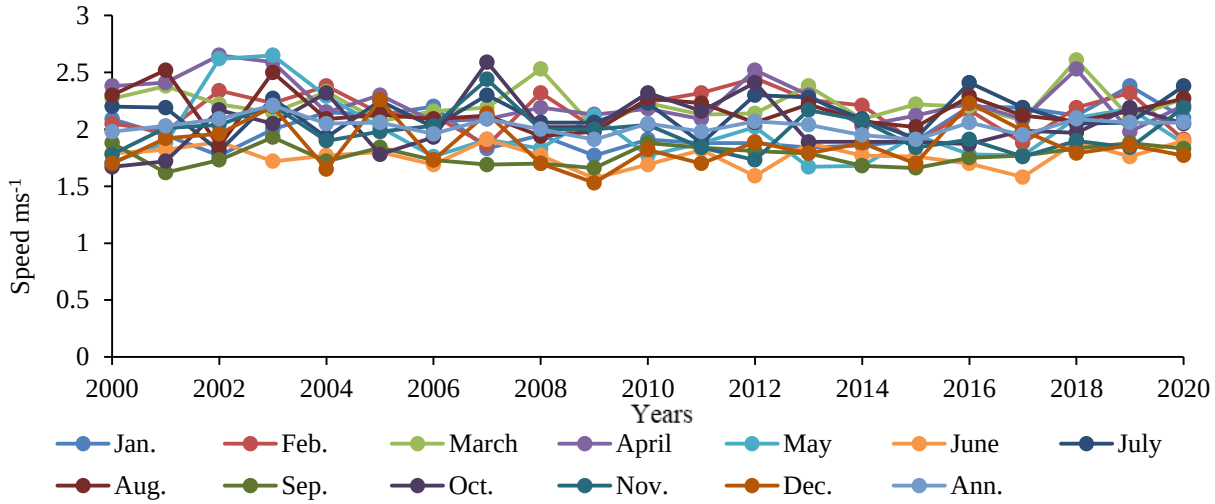

Figure 10. Wind speed

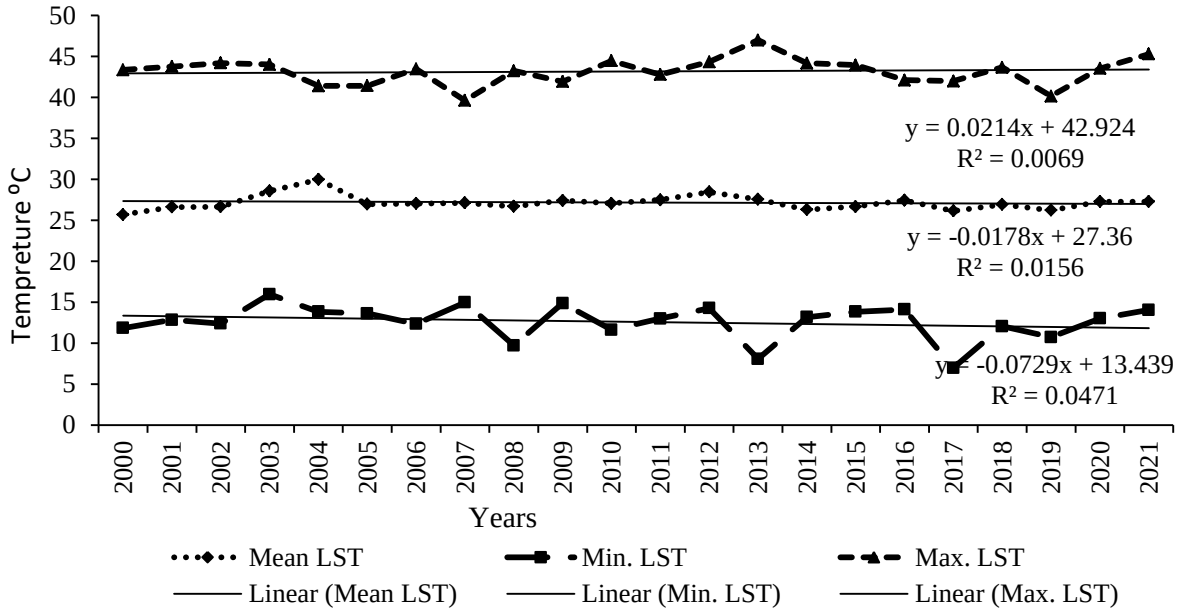

Figure 11. LST from MODIS data (2000-2021)

4 DISCUSSION

Increased human population and its influence on natural habitats are widespread worldwide, and it is more severe in developing countries. In the present attempt, the combined impacts of climate change and LULC on wetlands and surrounding environments. The relationship shows that both influence each other. It finds land use change with a decrease in forest and wetland areas. It has an unprecedented rate of land use changes over three decades. The results of the research indicated that the impact of LULC on the wetland and surrounding environment was greater than that of climate change impacts globally. Recent studies point out the importance of accounting for evolutionary process in forecasts of the future dynamics of LULC utility and LST trend was multi-directional (Wu *et al.*, 2017; Mendoza-Ponce *et al.*, 2018; Wang and Stephenson, 2018). For example, it reported that the earlier the change point, the smaller the relative contribution of climate change and the larger the relative contribution of human activities. However, there is an interaction between climate change and LULC. Climatic variables affect LULC, and in turn LULC affects regional climate (Li *et al.*, 2013). The coupled climatic variables, LULC types, and environmental change models are complex and complicated by the interactions

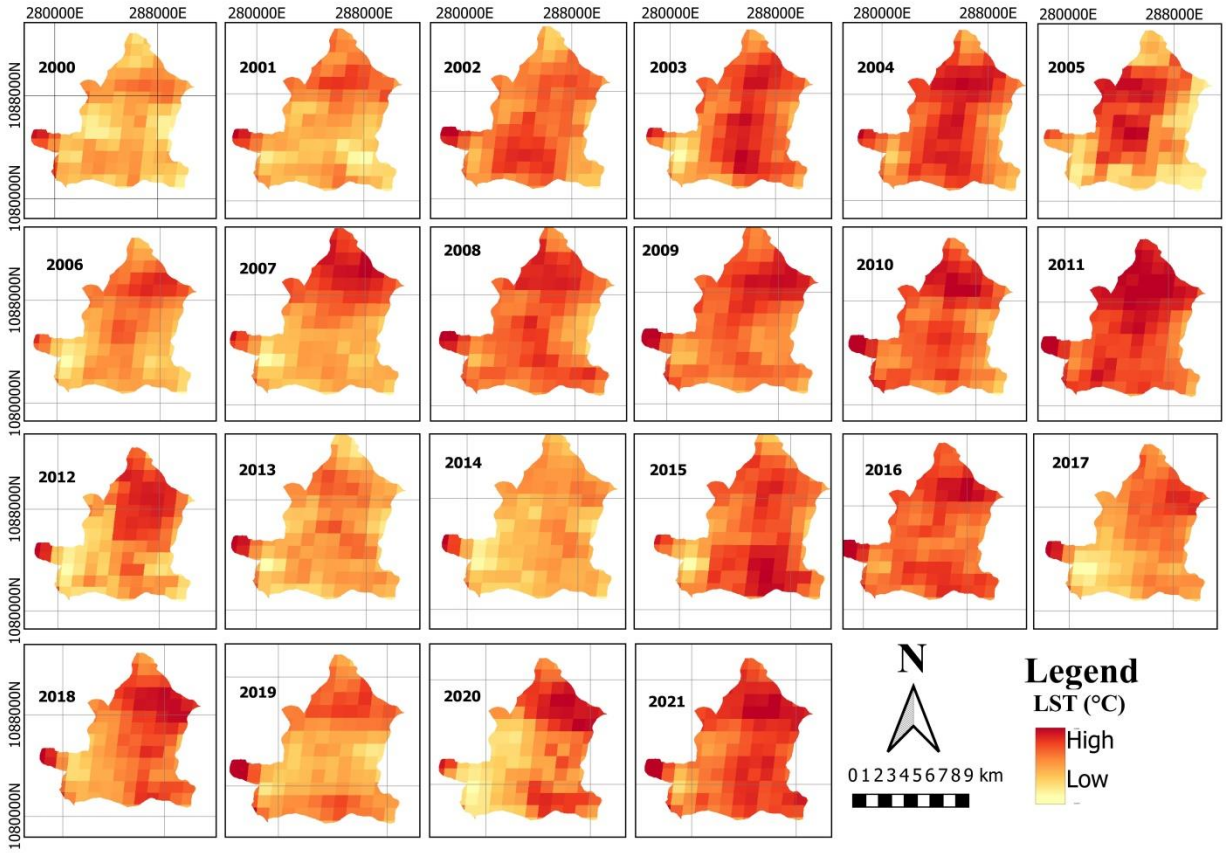

Figure 12. Distribution of LST

Table 7. Mean, minimum and maximum land surface temperature during (2000-2021)

Years	Mean LST	Min. LST	Max. LST
2000	25.68	11.84	43.35
2001	26.61	12.84	43.76
2002	26.64	12.39	44.19
2003	28.57	15.95	44.01
2004	29.97	13.83	41.39
2005	26.96	13.62	41.42
2006	27.03	12.35	43.47
2007	27.12	14.97	39.61
2008	26.69	9.715	43.23
2009	27.40	14.87	41.92
2010	27.06	11.63	44.47
2011	27.48	12.99	42.78
2012	28.45	14.26	44.32
2013	27.54	8.06	46.99
2014	26.29	13.16	44.18
2015	26.67	13.82	43.94
2016	27.43	14.11	42.10
2017	26.13	6.97	41.98
2018	26.92	12.06	43.67
2019	26.22	10.73	40.15
2020	27.28	13.01	43.52
2021	27.28	14.04	45.28

and feedback between subsystems through physical processes that separate the individual impacts of climate change and LULC on the surrounding wetland ecosystems from their combined impacts. In this study, the expansion of agricultural land-induced LULC, directly and indirectly, affects regional climate.

During this study, year 2015 revealed that farmland, plantation and grassland show increasing in 4510.8 ha, 591.3 ha and 976.5 ha, respectively, while forest, wetland and shrubland are decreased to 1291.4 ha, 505.8 ha and 237.5 ha, respectively. These results showed as the wetlands, forests and shrubland in the study area are not controlled by any authority and it is like 'free area' for any activity; hence, those inhabitants of the area that can work on farm moved in to produce mostly teff and Guizotia crops. Therefore, the main causes for resource losses in the study area sites are population growth, illegal cutting of forests for energy especially charcoal and firewood, and weak environmental laws and policies. This is comparable to the findings made by Olson *et al*. (2004) in Uganda.

Present results are in conformity several previous inferences in the study (Tadesse *et al*., 2017; Tafesse and Suryabhagavan, 2019; Bekele *et al*., 2022). On the other hand, farmland and plantation are increased to 4700.91 ha and 1585.32 ha, respectively, while others like, shrubland, grassland, wetland and forest decreased to 385.3 ha, 295.17 ha, 289.29 ha and 859.04 ha, respectively. The reasons for farmland and plantation increasing during this period are eucalyptus trees are used as the main source of fire wood for both rural and urban populations, expansion of rural and urban settlement, increasing price of eucalyptus trees, increasing number of unemployment, expansion of irrigation, population growth, weak land management and environmental policy implementation, lack of wise use and irresponsible for natural resource conservation in the area. As evident from the results of this work correspond to similar trends were identified of a study done in wetland uses and dynamics for agricultural purposes and its health implications in lower Ogun River basin, Lagos, Nigeria (2013). Climate and land-use change impacts are similar to countries like Ethiopia, India, Europe, and Africa.

Some studies have shown that the LST algorithm has excluded atmospheric radiation information, and the influence of atmospheric composition on LST no longer needs to be considered when analysing factors affecting LST (Tafesse and Suryabhagavan, 2019; Bekele *et al*., 2022). The relationship between LULC and LST is complex and multidirectional as land use change has been demonstrated to influence climate at local, regional, and global scales. However, the LST difference is affected not only by the difference in solar radiation but also by the surface cover, human activities, precipitation, airflow, and landscape pattern. Future research must consider factors such as airflow, monsoons, rainfall, solar radiation, seasonal climate change, and landscape patterns (Jiang et al. 2006; Li *et al*., 2013; Assaye *et al*., 2017). The quantitative relationship between each factor and temperature needs to be established and the mathematical model needs to simulate climate change. More thorough and detailed studies are needed to understand the dynamic mechanisms of climate change in the Jarmet Wetland and its surrounding environments and further assess human activities' impact on regional climate change.

5 CONCLUSION

The important objective of this study was to assessment LULC changes and its impact on climate change in Jarmet wetland and its surrounding environment using RS and GIS. The analysis of wetland and its surrounding environment indicated the dynamic change of LULC of the study area over years. The link between human development, illegal land use, weak resource conservation policy, and unwise use of wetland and other land cover recession can be measured through image classification, given that data is available and affordable for researches. In addition, the LULC dynamics is a result of complex interactions between several biophysical and socio-economic drivers. The effects of human activities are immediate and often radical, while the natural effects take a relatively longer period of time. The LULC change experienced in the area indicates the pressure on wetland, shrubland, grassland and forest cover and related biodiversity. Generally, the trends of wetlands, grassland, shrubland and forests are declining. It will create health, economic, and environmental problems for the Jarmet wetland if this changing rate of LULC and LST goes upwards in the upcoming years. This study will help improving the capacity of the government in the study area to device complete strategies at the local and national level for land management. Future researchers may give attention to the microclimatic change in the Jarmet wetland and ecological monitoring.

CONFLICT OF INTEREST

No conflict of interest exists to publish the article.

ACKNOWLEDGEMENTS

We are thankful to the School of Earth Sciences, and Department of Geography and Environmental studies, Addis Ababa University for support and facilities. We are also grateful to the Geospatial Information institute, Ethiopian Geological Survey, National Meteorological Service Agency, Central Statistical Agency and Alibo Bureau of Agriculture for their support in this study. We also thank two anonymous reviewers for the helpful suggestions.

ABBREVIATIONS

LULC: Land-use and land-cover; **Ha**: Hectare; **LST**: Land Surface Temperature.

REFERENCES

Al-Naimi, N., Raitsos, D.E., Ben-Hamadou, R., and Soliman, Y., 2017. Evaluation of Satellite Retrievals of

Chlorophyll-a in the Arabian Gulf. *Remote Sens*. 9, 301. DOI: https://doi.org/10.3390/rs9030301

Assaye, R., Suryabhagavan, K. V., Balakrishnan, M. and Hameed, S., 2017. Geo-spatial approach for urban green space and environmental quality assessment: a case study in Addis Ababa City. *J. Geogr. Inf. Syst*., 9, 191-206. DOI: https://doi.org/10.4236/jgis.2017.92012

Awoniran, D., Adewole, M., Adegboyega, S. and Anifowose, A., 2013. Assessment of environmental responses to land use-land cover dynamics in the Lower Ogun River Basin, Southwestern Nigeria. *African Journal of Environmental Science and Technology*. 8(2), 152-165. DOI: https://doi.org/10.5897/AJEST2013.1607

Ayele, K. F., Suryabhagavan, K. V., and Sathishkumar, B., 2014. Assessment of Habitat Changes in Holeta Watershed, Central Oromiya, Ethiopia. *International Journal of Earth Sciences and Engineering*. 7, 1370-1375.

Bekele, N. K., Hailu, B.T., and Suryabhagavan, K.V., 2022. Spatial patterns of urban blue-green landscapes on land surface temperature: A case of Addis Ababa, Ethiopia. *Current Research in Environmental Sustainability*, 4, 100146. DOI: https://doi.org/10.1016/j.crsust.2022.100146

Belete, T., and Suryabhagavan, K. V., 2019. Systematic Modeling of impacts of land-use and land-cover changes on land surface temperature in Adama Zuria District, Ethiopia. *Modeling Earth Systems and Environment*. 5, 805-817. DOI: https://doi.org/10.1007/s40808-018-0567-1

Chunqiao, S., Huang, B., Linghong, K., Richards, K. S. 2014. Remote sensing of alpine lake water environment changes on the Tibetan Plateau and surroundings: A review. *ISPRS Journal of Photogrammetry and Remote Sensing*. 92, 26-37. DOI: https://doi.org/10.1016/j.isprsjprs.2014.03.001

Chuvieco, E., and Kasischke, E.S., 2007. Remote sensing information for fire management and fire effects assessment. *J. Geophysics. Res.*, 112, G01S90. DOI: https://doi.org/10.1029/2006JG000230

Congalton, R. and Green, K., 2009. Assessing the Accuracy of Remotely Sensed Data. Principles and Practices. 2nd Edition. CRC/Taylor and Francis, Boca Raton, FL 183.

Congalton, R., 1991. A Review of Assessing the Accuracy of Classifications of Remotely Sensed Data. *Remote Sensing of Environment*. 37, 35-46. DOI: https://doi.org/10.1016/0034-4257(91)90048-B

Costanza, R., De Groot, R., Sutton, P., Ploeg, S., Anderson, S. J., Kubiszewski, I., Farber, S., and Turner, R. K., 2014. Changes in the global value of ecosystem services. *Global Environ. Change*, 26, 152-158. DOI: https://doi.org/10.1016/j.gloenvcha.2014.04.002

Dinku, S., and Suryabhagavan, K. V., 2019. Forest degradation monitoring and assessment of biomass in Harenna Buluk District, Bale Zone, Ethiopia: A geospatial perspective. *Trop Ecol*., 60, 94-104. DOI: https://doi.org/10.1007/s42965-019-00012-5

Dugan, P., 1993. Wetlands in Danger. *Oxford University Press*. New York, NY, USA.

Edwards, A. C., Rrssell-Smitha, J. and Maier, S. W., 2016. A comparison and validation of satellite-derived fire severity mapping techniques in fire prone north Australian savannas: Extreme fires and tree stem mortality. *Journal of Remote Sensing of Environment*, 206, 287-299. DOI: https://doi.org/10.1016/j.rse.2017.12.038

Edwards, T.C. Jr., Moisen, G.G., and Cutler, D. R., 1998. Assessing map accuracy in a remotely sensed, ecoregion-scale cover map. *Remote Sensing of Environment*. 63, 73-83. DOI: https://doi.org/10.1016/S0034-4257(96)00246-5

EPA [Environmental Protection Authority] 2004. Proceeding of the national workshop on the Ramsar Convention and Ethiopia. Addis Ababa,130.

Falcucci, A., Luigi, M., Luigi, B., 2007. Changes in land-use-land-cover patterns in Italy and their implications for biodiversity conservation. *Journal of Landscape Ecology*. 22, 617-631. DOI: https://doi.org/10.1007/s10980-006-9056-4

FAO [Food and Agriculture Organization] 2003. Livestock's long shadow. 00153 Rome, Italy.

FAO [Food and Agriculture Organization] 2016. Map Accuracy Assessment and Area Estimation, A Practical Guide, Rome, Italy. Food and Agriculture Organization of the United Nations (FAO). *National forest monitoring assessment working paper*, 46/E.

Finlayson, M., and Moser. M., 1991. Wetlands. International Waterfowl and Wetlands Research Bureau. *Facts on File Ltd*. Oxford, UK, 224.

Foody, G. M., 2002. Status of land cover classification accuracy assessment. *Remote Sens Environ*, 80,185-201.

Gao, Y., and Zhang, W., 2009. LULC classification and topographic correction of Landsat-7 ETM? imagery in the Yangjia River Watershed: The influence of DEM resolution. *Sensors*, 9, 1980-1995. DOI: https://doi.org/10.3390/s90301980

Gomez, C., White, J. C., and Wulder, M. A., 2016. Optical remotely sensed time series data for land cover classification: A review. *ISPRS Journal of Photogrammetry and Remote Sensing*, 116, 55-72. DOI: https://doi.org/10.1016/j.isprsjprs.2016.03.008

Gumma, M. K., Thenkabail, P. S., Hideto, F., Nelson, A., Dheeravath, V., Busia, D. and Rala, A., 2011. Mapping irrigated areas of Ghana using fusion of 30m and 250m resolution remote-sensing data. *Remote Sensing*, 3(4), 816-835. DOI: https://doi.org/10.3390/rs3040816

Helmer, E. H., Brown, S. and Cohen, W. B., 2000. Mapping montane tropical forest successional stage and land use with multi-date Landsat imagery. *International Journal of Remote Sensing*, 21, 2163-2183. DOI: https://doi.org/10.1080/01431160050029495

Jensen, J. R., 2005. Introductory Digital Image Processing, A Remote Sensing Perspective 3rd Edition. Prentice Hall, Upper Saddle River, NJ, USA.

Jensen, J. R., 2007. Remote Sensing of the Environment: An Earth Resource Perspec-tive, Upper Saddle River, NJ: Pearson Prentice-Hall, 592.

Jia, K., Wei, X., Gu, X., Yao, Y., Xie, X., and Li, B., 2014. Land cover classification using Landsat 8 Operational Land Imager data in Beijing, China. *Geocarto Int*., 29, 941-951. DOI: https://doi.org/10.1080/10106049.2014.894586

Jiang, G. M., Li, Z.L., and Nerry, F., 2006. Land Surface Emissivity Retrieval from Combined mid-Infrared and Thermal Infrared Data of MSG-SEVIRI. *Remote Sensing of Environment*, 105(4), 326-340. DOI: https://doi.org/10.1016/j.rse.2006.07.015

Lambin, E. F., and Geist, H., 2006. Land-Use and Land-cover Change on Local Processes and Global Impacts. *Springer Verlag Berlin Heidelberg*. Printed in Germany, 236.

Lellisand, M. T., Kiefer, R. W., and Chipman, J. W., 2004. Remote Sensing and Image Interpretation, Singapore. John Wiley and Sons, Pvt. Ltd.

Lesschen, J. P., Verburg, P. H., and Staal, S. J., 2005. Land-Use and Land-Cover Change (LUCC) Project. IV. *International Human Dimensions Programme on Global Environmental Change (IHDP) V*. International Geosphere Biosphere Programme (IGBP). International Livestock Research Institute, Kenya.

Li, G. G., Zhang, F., Jing, Y., Liu, Y., and Sun, G., 2017. Response of Evapotranspiration to Changes in Land Use and Land Cover and Climate in China during 2001-2013. *Sci. Total Environ*. 596-597, 256-265. DOI: https://doi.org/10.1016/j.scitotenv.2017.04

Li, J., Carlson, B. E., and Lacis, A. A., 2009. A study on the temporal and spatial variability of absorbing aerosols using total ozone mapping spectrometer and ozone monitoring instrument aerosol index data. *J. Geophysics. Res.*, 114, D09213. DOI: https://doi.org/10.1029/2008JD011278

Li, Z. L., Tang, B. H., Wu, H., Ren, H. Z., Yan, G. J., Wan, Z. M., Trigo, I. F., and Sobrino. J. A., 2013. Satellite-derived land surface temperature: Current Status and Perspectives. *Remote Sensing of Environment*, 131, 14-37. DOI: https://doi.org/10.1016/j.rse.2012.12.008

Lillesand, T., Kiefer, RW., and Chipman, J., 2015. Remote sensing and image interpretation. Wiley, New York.

Lu, D., and Weng, Q., 2007. A survey of image classification methods and techniques for improving classification performance. *International Journal of Remote Sensing*, 28(5), 823-870. DOI: https://doi.org/10.1080/01431160600746456

Lu, D., Hetrick, S., Moran, E., and Li, G., 2012. Application of time series landsat images to examining land-use/landcover dynamic change. *Photogramm Eng Remote Sens*., 78, 747-755. DOI: https://doi.org/10.14358/pers.78.7.747

Macleod, R. D., and Congalton, R. G., 1998. A quantitative comparison of change-detection algorithms for monitoring eelgrass from remotely sensed data. *Photogrammetric Engineering and Remote Sensing*. 64, 207-216.

Mekash, S. T., Suryabhagavan, K. V., and Kassawmar, T., 2022. Geospatial modelling of forest cover dynamics and impact of climate variability in Awi Zone, Ethiopia. *Tropical ecology*. 63,183-199. DOI: https://doi.org/10.1007/s42965-021-00199-6

Mekasha, S. T., Suryabhagavan, K. V., and Gebrehiwot, M., 2020. Geo-spatial approach for land-use and land-cover changes and deforestation mapping: A case study of Ankasha Guagusa, Northwestern, Ethiopia. *Tropical ecology*. 61, 550-569. DOI: https://doi.org/10.1007/s42965-020-00113-6

Melekneh, G., Suryabhagavan, K.V., and Balakrishnan, M., 2010. Land-use and landscape pattern changes in Holeta-Berga Watershed, Ethiopia. *International Journal of Ecology and Environmental Sciences*. 36, 117-132.

Mendoza, P., A., Corona-Núñez, R., Kraxner, F., Leduc, S., and Patrizio, P., 2018. Identifying Effects of Land Use Cover Changes and Climate Change on Terrestrial Ecosystems and Carbon Stocks in Mexico. *Glob. Environ. Change*, 53, 12-23. DOI: https://doi.org/10.1016/j.gloenvcha.2018.08.004

Misrak, A., Suryabhagavan, K. V., and Balakrishnan, M., 2012. Assessment of Cover Change in the Harenna Habitats in Bale Mountains, Ethiopia, Using GIS and Remote Sensing, *International Journal of Ecology and Environmental Sciences*. 38, 39-45.

Mitsch, W. J. and Gosselink, J. G., 1993. The value of wetlands: Importance of scale and landscape setting. *Ecological.Economics*. 35, 25-33. DOI: https://doi.org/10.1016/S0921-8009(00)00165-8

Moser, G. D., Tuia., L. Gomez Chova., and Camps Valls, G., 2015. Multimodal Classification of Remote Sensing Images. A Review and Future Directions. *IEEE*. DOI: https://doi.org/10.1109/JPROC.2015.2449668

NMSA [National Mission for Sustainable Agriculture] 2019. National Mission for Sustainable Agriculture (NMSA).

Olofsson, P., Foody, G. M., Stehman, S. V., and Woodcock, C. E., 2013. Making better use of accuracy data in land change studies: Estimating accuracy and area and quantifying uncertainty using stratified estimation. *Remote Sens Environ*, 129,122-131. DOI: https://doi.org/10.1016/j.rse.2012.10.031

Olsen, A., Bellerby, R.G.J., Johannessen, T., Omar, A.M., and Skjelvan, I., 2003. Interannual variability in the wintertime air- Sea flux of carbon dioxide in the northern North Atlantic, 1981-2001. *Deep Sea Research* I, 50, 1323-1338. DOI: https://doi.org/10.1016/S0967-0637(03)00144-4

Olson, J.M., Misana, S., Campbell, D.J., Mbonile, M., and Mugisha, S., 2004. The spatial pattern and root causes of land use changes in East Africa. LUCID Project Working Paper 47, International Livestock Research Institute, Nairobi.

RCW [Ramsar Convention on Wetlands] 2018. Ramsar Convention on Wetlands, Global Wetland Outlook: State of the World's Wetlands and Their Services to People. Ramsar Convention Secretariat, Gland, Switzerland.

Richards, J. A., 2013. Supervised Classification Techniques. In: Remote Sensing Digital Image Analysis. Springer, Berlin, Heidelberg. DOI: https://doi.org/10.1007/978-3-642-30062-2_8

Roy, M. B., Samal, N. R., Roy, P.K. and Mazumdar, A., 2010. Human wetland dependency and socio-economic evaluation of wetland functions through participatory approach in rural India. *Water Science and Engineering*, 3(4), 467-479. DOI; https://doi.org/10.3882/j.issn.1674-2370.2010.04.009

Sabins, F. F., 1997. Remote Sensing, Principals and Interpretation. New York: W.H. Freeman and Company. 494.

Serra, P., Pons, X. and Saurí, D., 2008. Land-cover and land-use change in a mediterranean landscape: A spatial analysis of driving forces integrating biophysical and human factors. *Applied Geography*, 28(3), 189-209. DOI: https://doi.org/10.1016/j.apgeog.2008.02.001

Shalaby, A. and Tateishi, R., 2007. Remote sensing and GIS for mapping and monitoring land cover and land-use changes in the Northwestern Coastal Zone of Egypt. *Applied Geography*, 27, 28-41. DOI: https://doi.org/10.1016/j.apgeog.2006.09.004

Sruthi, S. and Mohammed, A., 2015. Agricultural Drought Analysis Using the NDVI and Land Surface Temperature Data; A Case Study of Raichur District. *Aquatic Procedia*, 4, 1258-1264. DOI: https://doi.org/10.1016/j.aqpro.2015.02.164

Suryabhagavan, K. V., 2017. GIS-based climate variability and drought characterization in Ethiopia over three decades. *Weather and Climate Extremes*. 15, 11-23. DOI: https://doi.org/10.1016/j.wace.2016.11.005

Tadesse, L., Suryabhagavan, K.V., Sridhar, G., and Legesse, G., 2017. Landuse and landcover changes and Soil

erosion in Yezat Watershed, North Western Ethiopia. *International Soil and Water Conservation Research*. 5, 85-94. DOI: https://doi.org/10.1016/j.iswcr.2017.05.004

Tegene, B., 2002. Land-Cover-Land-Use Changes in the Derekolli Catchment of the South Welo Zone of Amhara Region, Ethiopia. *Eastern Africa Social Science Research Review*, 18, 1-20. DOI; https://doi.org/10.1353/eas.2002.0005

Turner, B. L., Meyer, W. B., and Skole, D. L., 1994. Global land-use/land-cover change towards an integrated study. *Ambio*. 23, 91-95.

USGS [United States Geological Survey] 1992. Multi-resolution land characteristics-state wide digital data for Mississipi.

Verma, P., Raghubanshi, A., Srivastava, P.K., Raghubanshi, A. S., 2020. Appraisal of kappa-based metrics and disagreement indices of accuracy assessment for parametric and nonparametric techniques used in LULC classification and change detection. *Model Earth Syst Environ*., 6, 1045-1059. DOI: https://doi.org/10.1007/s40808-020-00740-x

Wan, Z., Wang, P., and Li. X., 2004. Using MODIS Land Surface Temperature and Normalized Difference Vegetation Index Products for Monitoring Drought in the Southern Great Plains, USA. *International Journal of Remote Sensing*, 25 (1), 61-72. DOI: https://doi.org/10.1080/0143116031000115328

Wang, H., and Stephenson, S.R., 2018. Quantifying the impacts of climate change and land use/cover change on runoff in the lower Connecticut river basin. *Hydrol. Process*. 32 (9), 1301-1312. DOI: https://doi.org/10.1002/hyp.11509

Wang, T. L., Zhou, L. F., and Yang, P. Q., 2008. Study of Panjin wetlands along Bohai Coast. The information System of wetlands based on 3S technique. *Journal of Ocean University of China (English Edition)*,7(4), 411-415.

Warkaye, S., Suryabhagavan, K. V. and Satishkumar, B., 2018. Urban green areas to mitigate urban Heat Island effect: The case of Addis Ababa, Ethiopia. *Int. J. Ecol. Environ. Sci*., 44, 353-367.

WBISPP [Woody Biomass Inventory and Strategic Planning Project] 2005. A National Strategic Plan for the Biomass Energy Sector. *Ethiopia: Federal Ministry of Agriculture*. Addis Ababa.

WCED [World Commission of Environment and Development], 1987. Our Common Future. WCED. *Oxford University Press*. New York, USA, 398.

Wood, A. P., and Dixon A. B., 2002. Sustainable wetland management in Illubabor Zone. *Huddesfield*, UK: Huddesfield University.

Wu, J., Miao, C., Zhang, X., Yang, T., and Duan, Q., 2017. Detecting the Quantitative hydrological response to changes in climate and human activities. *Sci. Total Environ*. 586, 328-337. DOI: https://doi.org/10.1016/j.scitotenv.2017.02.010

Yuan, F., Sawaya, K. E., Loeffelholz, B. C., and Bauer, M. E., 2005. Land cover classification and change analysis of the Twin Cities (Minnesota) Metropolitan Area by multitemporal Landsat remote sensing. *Remote Sensing of Environment*, 98(2-3), 317-328. DOI: https://doi.org/10.1016/j.rse.2005.08.006

Zersenay, A., Jonathan, G., Wynn, D., Denne, R., W. Andrew, B., Rene, B., Shannon, P., McPherron, Alan D., Mulugeta, A., Mark J., Sier, Diana, R., and Joseph, M., 2020. Fossils from Mille-Logia, Afar, Ethiopia, elucidate the link between Pliocene environmental changes and Homo origins. *Journal of Nature Communications*, 11, 2480. DOI: https://doi.org/10.1038/s41467-020-16060-8

*****